KOMPETENZZENTRUM WasserBerlin

REPORT

Contract: COSMA-1, D 2.3
Final version, **Date: 27.06.2014**

Cicerostr. 24
D-10709 Berlin
Germany
Tel +49 (0)30 536 53 800
Fax +49 (0)30 536 53 888
www.kompetenz-wasser.de

Freie Universität Berlin

GFZ Helmholtz-Zentrum POTSDAM

Hydrogeological and static structural geological model implementation

- Modeling Scenarios -

COSMA-1, D 2.3

by

L. Thomas, T. Taute, M. Schneider (Freie Universität Berlin)

T. Kempka, M. Kühn (Deutsches GeoForschungsZentrum GFZ, Potsdam)

for

Kompetenzzentrum Wasser Berlin gGmbH

Preparation of this report was financed in part through funds provided by

VEOLIA WATER

VEOLIA ENVIRONNEMENT

Berlin, Germany

2014

Important Legal Notice

Disclaimer: The information in this publication was considered technically sound by the consensus of persons engaged in the development and approval of the document at the time it was developed. KWB disclaims liability to the full extent for any personal injury, property, or other damages of any nature whatsoever, whether special, indirect, consequential, or compensatory, directly or indirectly resulting from the publication, use of application, or reliance on this document. KWB disclaims and makes no guaranty or warranty, expressed or implied, as to the accuracy or completeness of any information published herein. It is expressly pointed out that the information and results given in this publication may be out of date due to subsequent modifications. In addition, KWB disclaims and makes no warranty that the information in this document will fulfill any of your particular purposes or needs. The disclaimer on hand neither seeks to restrict nor to exclude KWB's liability against all relevant national statutory provisions.

Wichtiger rechtlicher Hinweis

Haftungsausschluss: Die in dieser Publikation bereitgestellte Information wurde zum Zeitpunkt der Erstellung im Konsens mit den bei Entwicklung und Anfertigung des Dokumentes beteiligten Personen als technisch einwandfrei befunden. KWB schließt vollumfänglich die Haftung für jegliche Personen-, Sach- oder sonstige Schäden aus, ungeachtet ob diese speziell, indirekt, nachfolgend oder kompensatorisch, mittelbar oder unmittelbar sind oder direkt oder indirekt von dieser Publikation, einer Anwendung oder dem Vertrauen in dieses Dokument herrühren. KWB übernimmt keine Garantie und macht keine Zusicherungen ausdrücklicher oder stillschweigender Art bezüglich der Richtigkeit oder Vollständigkeit jeglicher Information hierin. Es wird ausdrücklich darauf hingewiesen, dass die in der Publikation gegebenen Informationen und Ergebnisse aufgrund nachfolgender Änderungen nicht mehr aktuell sein können. Weiterhin lehnt KWB die Haftung ab und übernimmt keine Garantie, dass die in diesem Dokument enthaltenen Informationen der Erfüllung Ihrer besonderen Zwecke oder Ansprüche dienlich sind. Mit der vorliegenden Haftungsausschlussklausel wird weder bezweckt, die Haftung der KWB entgegen den einschlägigen nationalen Rechtsvorschriften einzuschränken noch sie in Fällen auszuschließen, in denen ein Ausschluss nach diesen Rechtsvorschriften nicht möglich ist.

Colophon

Title
Final report: Hydrogeological and static structural geological model implementation - Modeling Scenarios; COSMA-1, D 2.3

Authors
L. Thomas, T. Taute, M. Schneider (Freie Universität Berlin)
T. Kempka, M. Kühn (Deutsches GeoForschungsZentrum GFZ, Potsdam)

Quality Assurance
H. Schwarzmüller (KWB)
N. Quisel (VERI)
B. David (VE DTO)

Publication / Dissemination approved by technical committee members
Boris David, Veolia Eau DT
Andreas Hartmann, KWB
Michael Kühn, GFZ
Michael Schneider, FUB
Emmanuel Soyeux, VERI

Deliverable number
D 2.3

Final version ☐
Date: 03.06.2014

Geological **CO_2 S**torage and Other E**m**erging Subsurface **A**ctivities
- Protection of Groundwater Resources

COSMA

Final Report

Hydrogeological and static structural geological model implementation

- Modeling Scenarios -

FU Berlin: L. Thomas, T. Taute, M. Schneider

GFZ, Potsdam: T. Kempka, M. Kühn

Contents

1 Introduction

The final report of the project COSMA describes the modeling results of four different scenarios regarding the pressure build-up in shallow aquifers due to the injection of CO_2 into the sandstone aquifers of the Detfurth Formation.

It is based on the "Technical Report on hydrogeological and static structural geological model implementation" (D 2.1) which focuses on the compilation of geological and hydrogeological background data (average values) and the development of a simplified conceptual hydrogeological model for a setting typical for the Northern German Sedimentary Basin as well as the model selection, model parameterization, definition of boundary conditions and implementation in hydrogeological flow model software packages.

The hydrogeological model of the Cenozoic includes Quaternary and Tertiary aquifers down to the layer beneath the Rupelian clay. Moreover, a concept for modeling the interaction between deep, consolidated, saline aquifers with unconsolidated freshwater aquifers was developed.

This report describes scenario analyses by using the numerical hydraulic model of the Detfurth Formation (Middle Bunter) and the simplified numerical groundwater model of the Cenozoic. The numerical models can be used to assess the key parameters, having an impact on the upconing of deeper saline groundwater beneath the well fields of water works (in shallow aquifer) due to imposed pressure signals.

2 Deep structural geological model

A deep structural geological model was implemented to account for subsurface underground utilization such as geological CO_2 storage in the scope of the research aims in the COSMA project. Two numerical modelling scenarios have been realized based on investigation of different approaches of coupling the shallow FUB and deep GFZ numerical models.

2.1 Detfurth Formation as potential reservoir

The Detfurth formation has a total thickness of 60 m and offers suitable conditions for e.g. CO_2 storage. The Detfurth sandstone is 23 m thick and the reservoir top of the chosen Mesozoic anticline at a depth of about 1,100 m (Fig. 1). 37 m of the Detfurth formation comprise a low permeable sequence which is located above the potential storage formation. Based on typical geometries the anticline is assumed to have an east-west extension of about

20 km and an extension with north-south orientation of 5 km. The Detfurth sandstone is parameterized by a porosity of 15 % to 18 % and a permeability of 200 mD to 600 mD (Vattenfall, 2009).

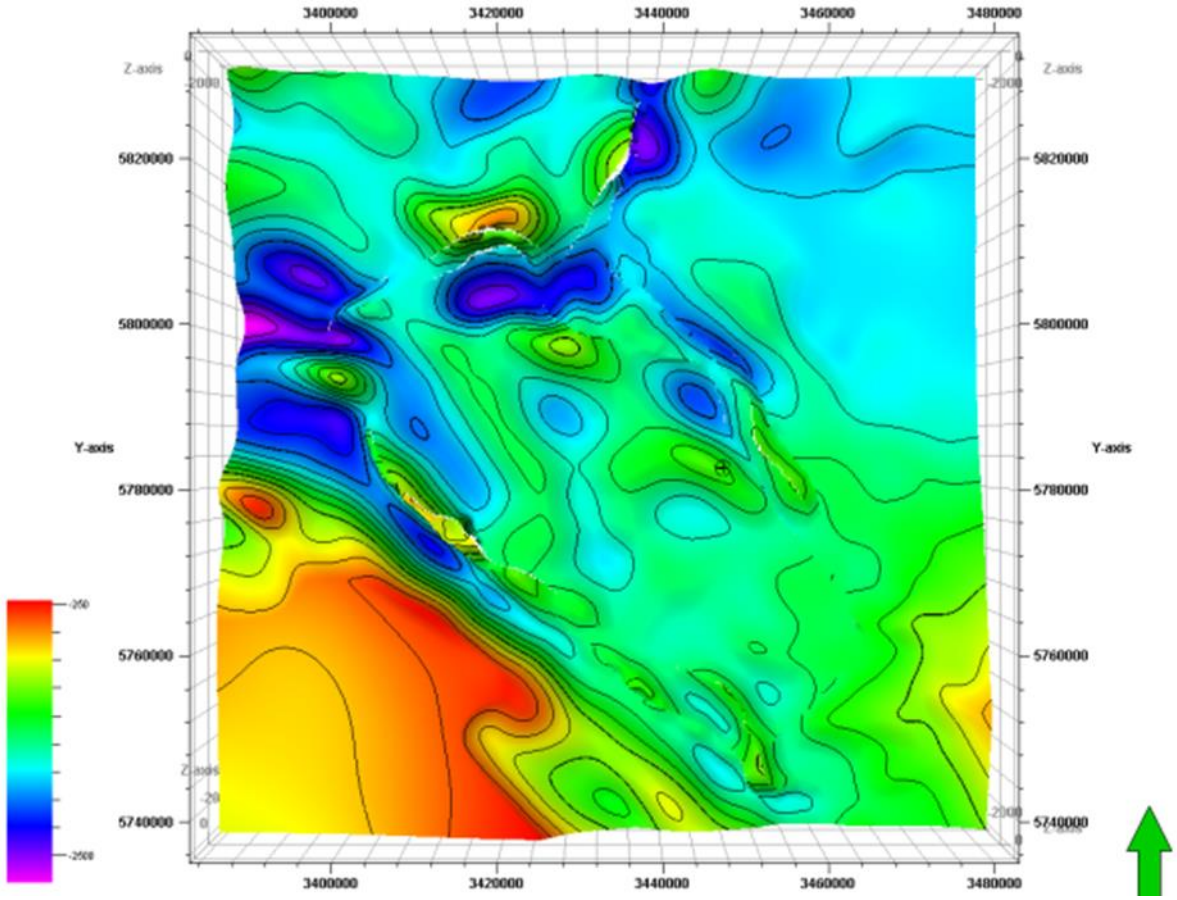

Fig. 1: 3D Structural geological model including the top horizon of Detfurth formation. Model 5x exaggerated.

2.2 Implementation of the structural geological model

The Petrel software package (Schlumberger, 2011) was used to build up the 3D structural geological model (Röhmann, 2013). For that purpose, depth contour lines of the Zechstein-Top (cf. Fig. 2) were imported and digitalized using the Petrel software package, and subsequently adjusted to the depth and thickness of the Detfurth formation (cf. Fig. 1). The modelling area has an areal extent of 100 km x 100 km and a maximum thickness of 1,700m. The 3D model includes the Detfurth storage formation as well as fault elements which extend to the base of the Rupelian clay (cf. Fig. 2).

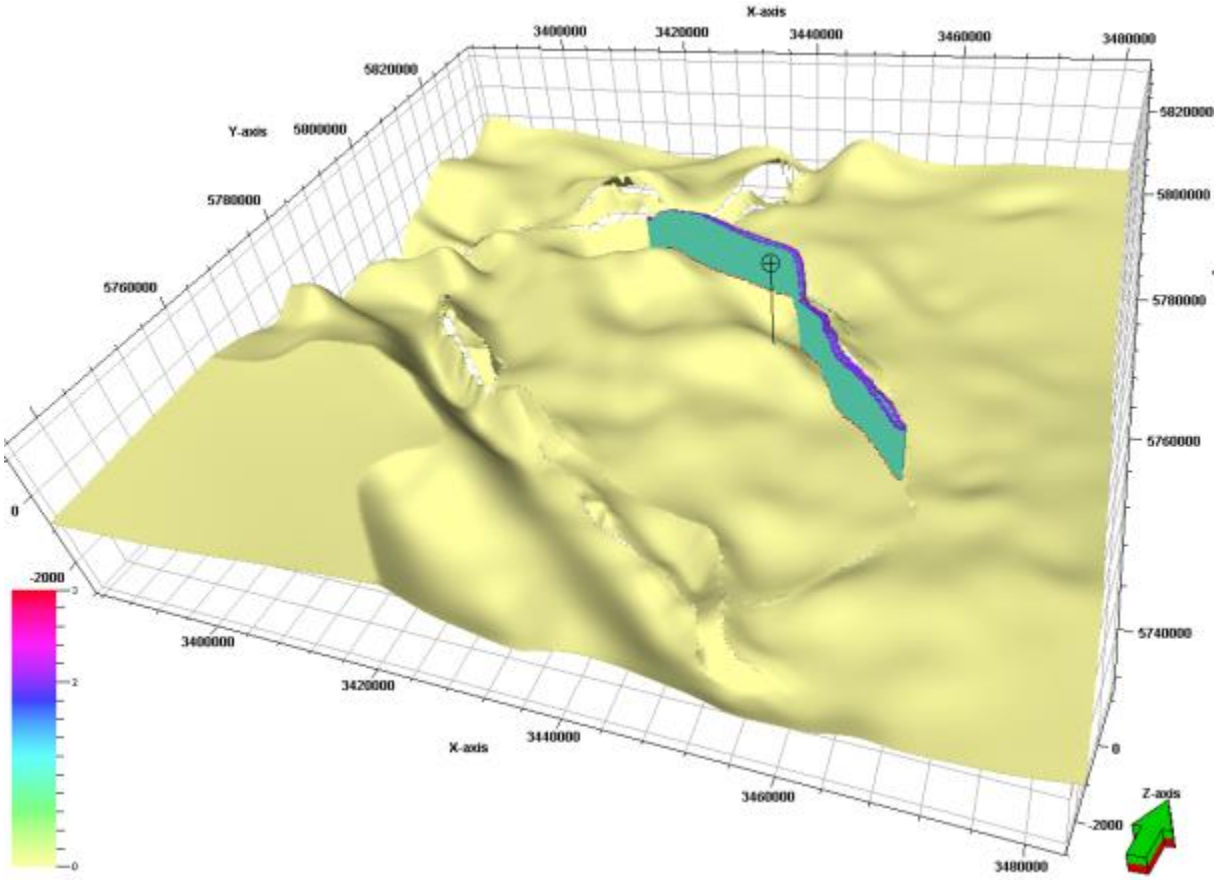

Fig. 2: 3D model with active elements (Detfurth formation and closest fault of the first fault system) as well as the position of the injection well, vertical exaggeration factor is 5).

2.3 Implementation of geological faults

The model comprises four fault systems which enclose the CO_2 selected injection site (cf. Fig. 3). One fault system is oriented NW-SE and situated about 5 km east of the southwest dipping anticline. Another fault zone extends west to the anticline and has the same orientation, but is dipping northeast. A third SW-NE orientated fault zone passes north of the anticline and is dipping southeast. South of the anticline is the fourth fault zone cutting the Northern German Sedimentary Basin. All fault systems are mostly constituted of normal faults, except of the first mentioned fault zone which features reverse faults in some parts (Röhmann et al., 2013).
A total of nine faults are considered in the study area. For the investigations all faults are expected as vertically impermeable, except the closest fault to the injection well (Fig. 2). This fault (length 120 km) is assumed to be located in the sphere of influence of the pressure elevation due to CO_2 injection in selected storage site. Permeable (400 mD, equals to about $4e^{-13}$ m^2) elements were set next to the fault to investigate potential upward brine migration through the fault zone.

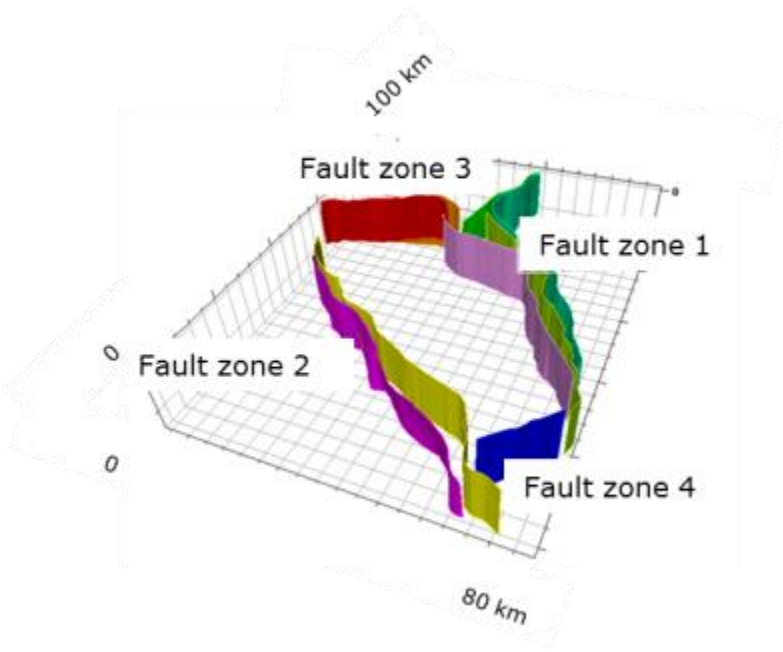

Fig. 3: Faults that build up the four fault systems enclosing the hypothetical CO_2 storage anticline (Röhmann, et al. 2013).

2.4 Revision of numerical model grid

In order to implement the 3D geological model into the multi-phase flow simulator it is necessary to discretize the geological model in respect to the general grid convergence criteria of the simulator. For this reason the model was initially gridded using the Petrel software package. To realize the workflow, the geometry of the structural framework was transferred to the gridding process including all geological horizons, additionally defining the grid increment (Röhmann et al., 2013). Hereby, a lateral discretisation of 250 m x 250 m with about 4.6 m (Detfurth formation) and about 28 m (fault elements) in vertical direction was assigned creating a 3D grid. This resulted in a total of 8.8 million elements (nx = 400, ny = 400, nz = 55), whereby 832,600 elements were determined as being active. The Detfurth formation contains 800,000 elements (nx = 400, ny = 400, nz = 5), while the fault is composed of 32,600 elements. Following a model revision based on initial coupling results (GFZ and FUB numerical models), the fault length was decreased to 2 km in order to account for the FUB model size (Figure 4). Thereby, the fault was discretized by about 800 elements.

Parameterization of salinity, temperature and pressure was carried out to implement a representable 3D model of the study area as discussed by Tillner et al. (2013). The distributions of these parameters are plotted in Fig. 4 and Table 1. Model boundaries are

assumed to be closed by implementation of the Neumann "no-flow" condition at the boundary elements, whereas the top elements of the fault were multiplied with a pore volume factor of 10^{10} in order to represent an overlying aquifer below the base of the Rupelian clay (Dirichlet boundary condition). The numerical model was equilibrated for a time of 10,000 years in order to achieve static flow conditions in the entire domain, whereas a salinity gradient was applied at the fault. The equilibrated model was then applied as initial state for the two scenarios investigated by GFZ.

	Permeability (m²)	**Porosity (%)**
Rupelian sands	$K_h = 1 \times 10^{-10}$	25
	$K_v = 1/3\ K_h$	
Fault system	1×10^{-12}	25
	$K_v = K_h$	
Detfurth Formation	$K_h = 4 \times 10^{-13}$	17
	$K_v = 1/3\ K_h$	

Table 1: Initial model parameterization

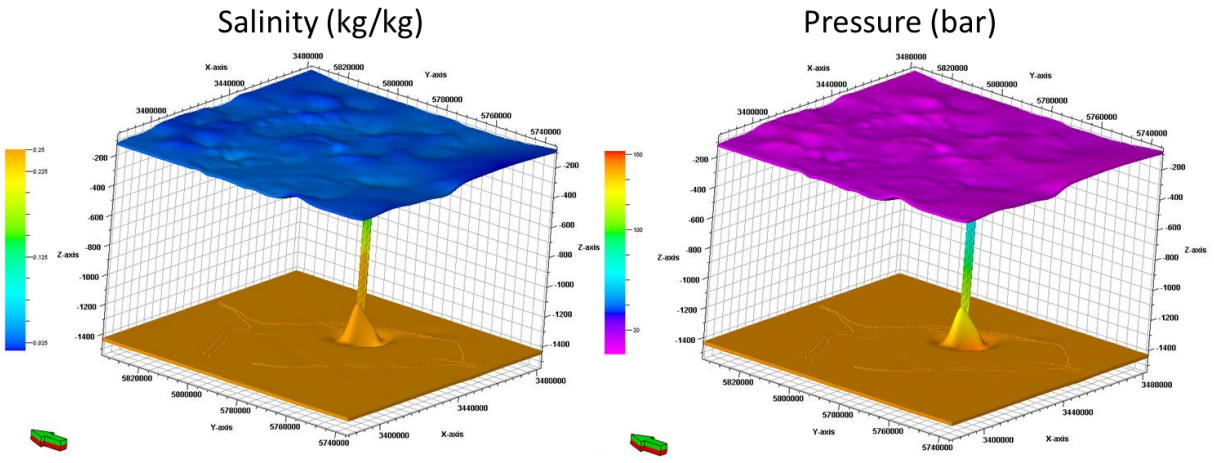

Fig. 4: Initial settings for the 3D model. Salinity (left) and pressure (right) (vertical exaggeration factor is 10).

2.5 Numerical simulation results

Using the equilibrated numerical model, two different scenarios were investigated considering a 2 km fault length close to the CO_2 injection location. 1.7 Mt CO_2/year were injected including a total of 65 kt brine/year in order to avoid salt precipitation in the near-well area that would induce local permeability decrease, and thus a significant reduction of CO_2 injectivity into the target formation. The lateral hydraulic conductivity of the faults located in the Detfurth Formation was set to the formation conductivity in the laterally open fault and to zero in the laterally closed fault scenario.

Simulation results show that the salinization footprint in the Rupelian sands is almost equal for both scenarios (Fig. 5). Nevertheless, the amount of displaced brine in the closed fault scenario is about twice as high compared to the open fault one (Fig. 7). Figure 6 shows the differential pressure for both scenarios, whereas the laterally open fault scenario pressure increase is about 1.5 MPa below that in the laterally closed fault scenario. Consequently, the higher pressure gradient between the Detfurth Formation and the Rupelian sands drives the upward displacement of additional brine.

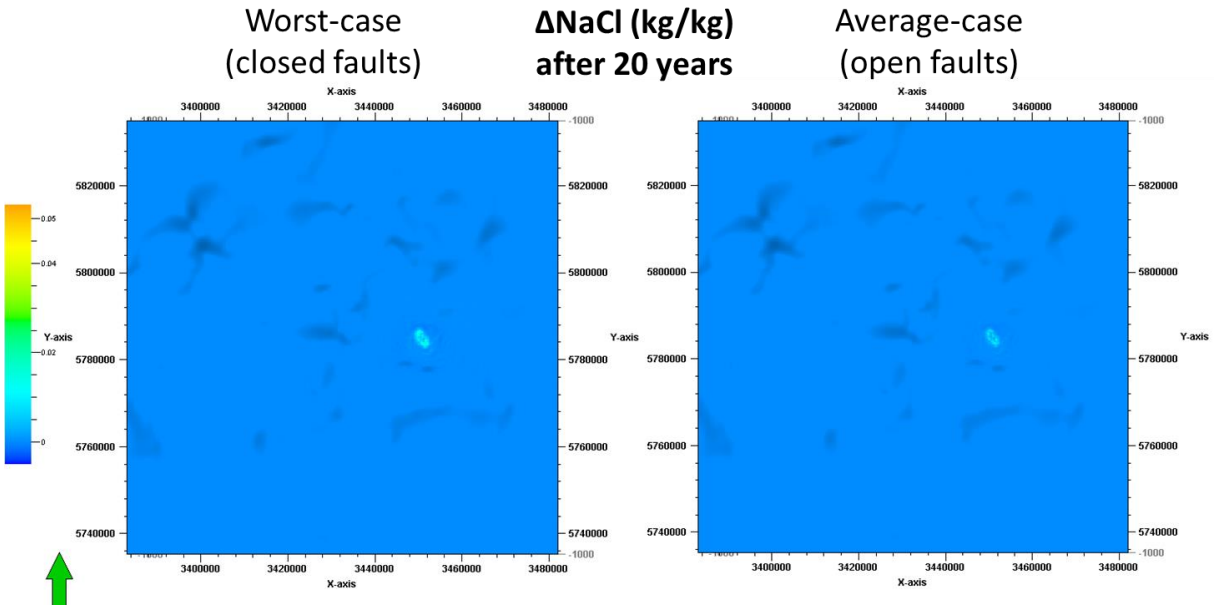

Fig. 5: Plane view of the Rupelian sands shows that spatial salinity increase (salinity footprint) is almost identical in both simulation scenarios after 20 years of CO_2 injection in the Detfurth Formation.

Figure 6 indicates that the pressure perturbation in the laterally closed fault scenario occurs up to the model boundaries of the closed fault scenario, while it is limited to the eastern model boundary in the open fault scenario, only.

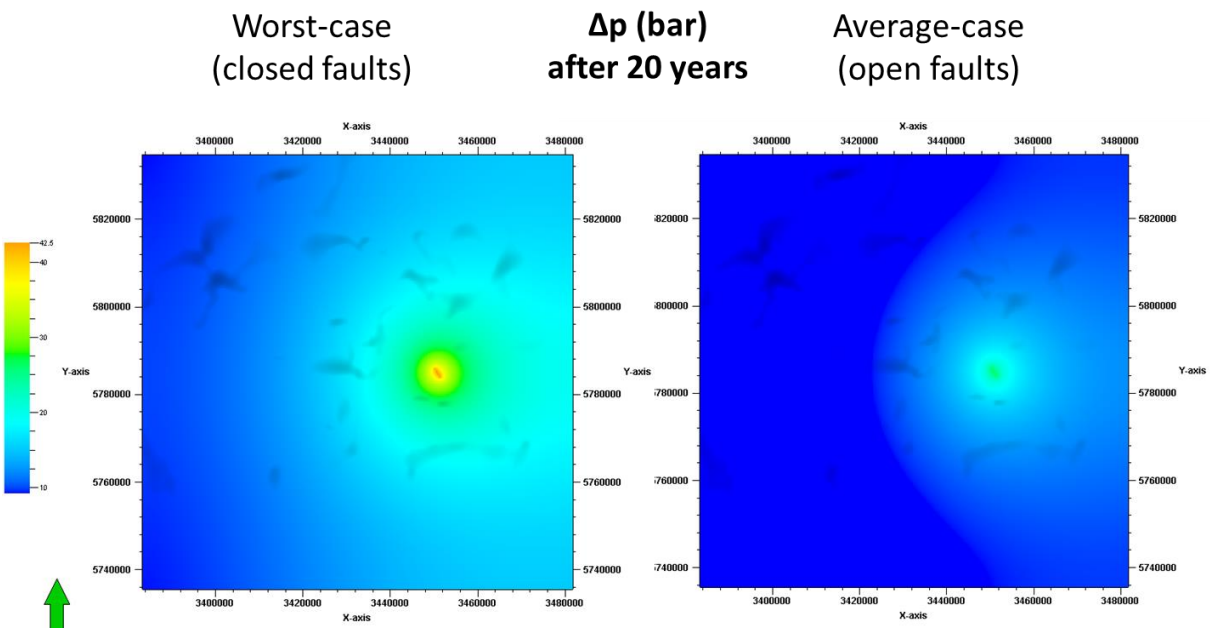

Fig. 6: Plane view of the Rupelian sands shows significant pressure difference of about 1.5 MPa between both scenarios.

Figure 7 plots the calculated H_2O and NaCl displacement over the entire simulation time of 20 years. Significantly more brine is displaced into the Rupelian sands in the closed fault scenarios as a result of the higher pressure gradient resulting from the reservoir compartementalization in the Detfurth Formation.

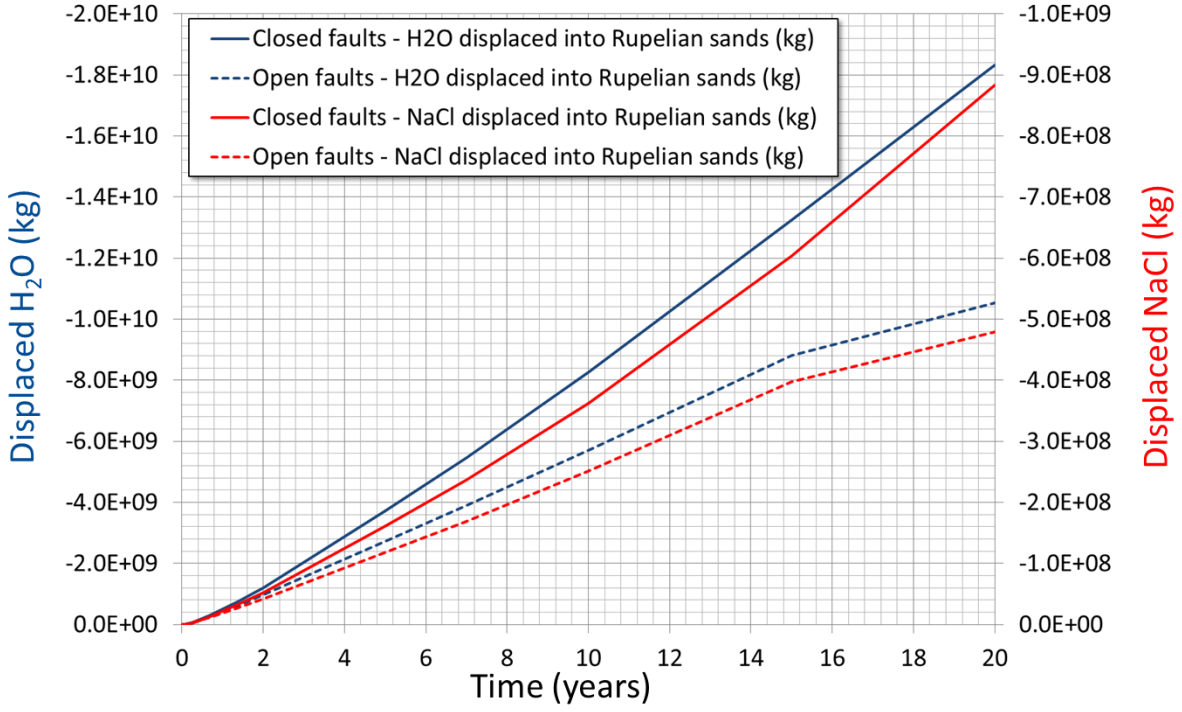

Fig. 7: Amount of displaced brine is about twice as high in the closed fault (worst-case) compared to the open fault scenario.

Figure 8 illustrates the pressure development at the injection well in the Detfurth Formation during CO_2 injection (20 years) and 80 years thereafter. Pressure elevation in the worst-case scenario is about 20 bar higher than in the average-case scenario.

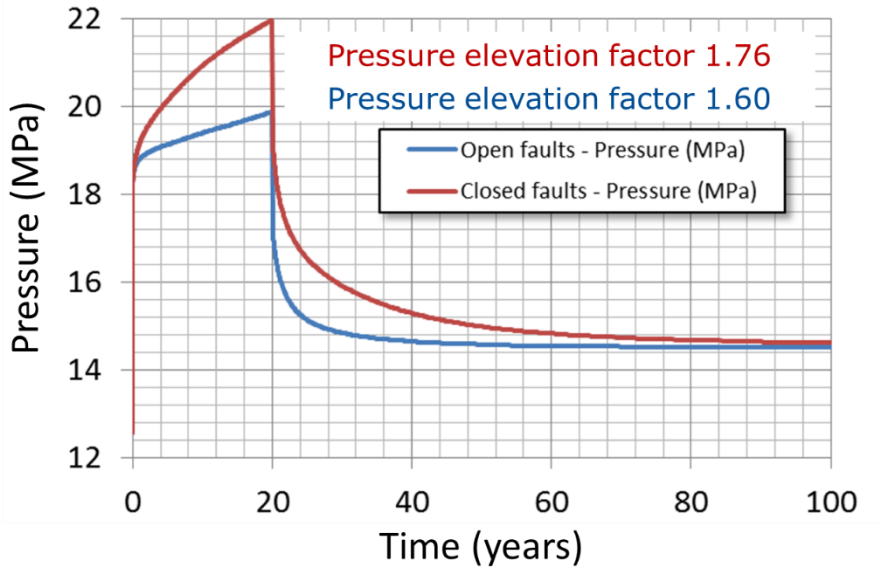

Fig. 8: Pressure development in the laterally open and closed faults scenarios at the CO_2 injection well in the Detfurth Formation.

In summary, we conclude that lateral conductivity of faults has a significant influence on brine migration in the two investigated scenarios. Spatial salinity increase in the Rupelian sands is limited to a radius of about 4 km around the leaky fault. Salinity increase and amount of displaced brine is about two times higher in the worst-case scenario. Local pressure in the Rupelian sands increases by about 42 bar in the worst- and about 26 bar in the average-case. A pressure increase by 95 bar in the Detfurth Formation results in a pressure elevation by 42.5 bar in the Rupelian sands in the worst-case scenario Hence, our numerical modelling results emphasize the importance of hydrogeological fault characterization in the scope of geological underground utilization.

3 Hydrogeological model of the Cenozoic

3.1 Conceptual model

The conceptual hydrogeological model of the Cenozoic contains the basic stratigraphic and lithologic units, which are characteristic of the Northern German sedimentary basin.

The hydrogeological model should represent a "worst case"- scenario, which includes hydraulic windows within the Rupelian clay as well as deep glacial erosion channels allowing an ascent of salt water into shallow freshwater aquifers. Therefore, the model does not represent the real situation within the deeper subsurface of a defined location, but possible geological conditions in the sense of worst-case scenarios. Nevertheless, stratigraphy, lithology and hydrogeological units of the model are typical for the Northern German Sedimentary Basin and derived from geological and stratigraphical profiles, drilling logs and literature (Gocht 1964, Frey 1975, Kloos 1986, Kallenbach 1980, 1993, Lippstreu 1995, Manhenke et al. 1995, 2001, Wurl 1995, Pekdeger et al. 1998, Limberg & Thierbach, 1997, 2001, Limberg et al. 2009). Based on these data, a conceptual hydrogeological model of a selected region with a model scale of 10 km x 10 km as a basis for a numerical model was created. This model includes Quaternary and Tertiary aquifers and aquicludes down to the layer beneath the Rupelian clay (Tab. 2).

Tab. 2: Schematic conceptual hydrogeological model with parameterization of the layers
(qh = Quaternary Holocene, qw = Quaternary Weichselian, qhol = Quaternary Holsteinian, tmi = Tertiary Miocene, tolCO = Tertiary Oligocene Cottbus layers, tolRA = Tertiary Oligocene Rupelian Basissand, teo = Tertiary Eocene, Jur = Jurassic, Cret = Cretaceous).

Model Layer	Hydraulic unit (Thickness)	Type	kf [m/s] (average)	Layer type	Strati-graphy
I	**GWL 1** (~ 25 m)	Aquifer	3.0E-03	unconfined	qw-qh
II	(~ 10 m)	Aquiclude	1.0E-09		
III	**GWL 2** (~ 50 m)	Aquifer	2.0E-03	confined / unconfined	qhol-qw
IV	(~ 10 m)	Aquiclude	1.0E-09		
V	**GWL 3** (~ 20 m – ~ 150 m)	Aquifer	6.0E-04	confined	tmi-qhol
VI	(~ 15 m)	Aquiclude	1,0E-09		
VII	**GWL 4** (~ 80 m)	Aquifer	6.0E-04	confined	tolCO-tmi
VIII	(~ 100 m)	Aquiclude (Rupelian)	1.0E-09		
IX	**GWL 5** (~10 m)	Aquifer	1.0E-04	confined	teo-tolRa Jur/Cret
X	(~ 50 m)	Aquiclude	1,0E-09		Jur/Cret

3.2 Implementation in a numerical model

The spatial data of the conceptual hydrogeological model were digitized using the program package SURFER (Golden Software, Inc.) and imported in ModFlow (USGS; Harbaugh 2005) as the basis for the numerical model (Fig. 9).

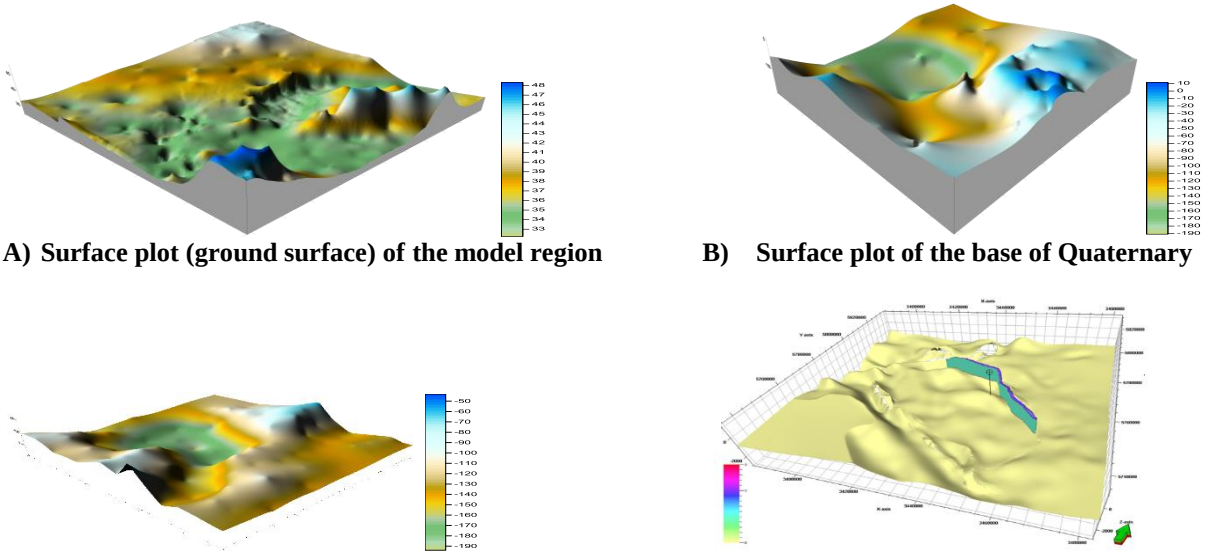

A) Surface plot (ground surface) of the model region

B) Surface plot of the base of Quaternary

B) Surface plot of the top of Rupelian clay (Layer 8 of the numerical model)

D) 3D model of the deeper underground

Fig. 9: Topography of different Layers for implementation in a numerical model (A-C) and 3-D model of the deeper underground (D) with fault system (Detfurth formation) and the position of the injection well. Deep structural model created by GFZ. All scales in m NN.

ModFlow uses a 3D finite differences numerical method. For computational reasons, the model was limited to an area of 10 km x 10 km. It contains a total of ten layers with five aquifers as hydraulic units, separated by five aquicludes (see Tab. 2). Since only worst case scenarios should be considered, the boundary conditions were set as no flow and closed conditions.

For implementing the 3D conceptual hydrogeological model into the numerical ModFlow software package, the Kriging method as the gridding tool was applied, using a linear semi-variogram model and an anisotropy ratio of 1. As a search method, octant with 1 data per sector was chosen. The grid size was defined as 100 m x 100 m, resulting in a total of 10.000 nodes. The parameterization of the different layers is shown in Tab. 3.

Tab. 3: Parameterization of the different layers in the numerical model

Model layer	Aquifer (GWL)	Horizontal hydraulic conductivity [m/s]	Vertical hydraulic conductivity [m/s]	Effective porosity (estimated)	Thickness [m]
I	1	3.0 E-03	3.0 E-04	0.25	25
II		1.0 E-09	1.0 E-10	0.05	10
III	2	2.0 E-03	2.0 E-04	0.25	50
IV		1.0 E-09	1.0 E-10	0.03	10
V	3	2.0 E-03	2.0 E-04	0.25	20-150
VI		1.0 E-09	1.0 E-10	0.03	15
VII	4	6.0 E-04	6.0 E-05	0.25	80
VIII		1.0 E-09	1.0 E-10	0.01	0-100
IX	5	1.0 E-04	1.0 E-05	0.25	10

3.3 Model refinement and model coupling

A first numerical model was created with the software package Processing Modflow, Version 5.3.1 (PMWin 5.3.1, 2001; Chiang & Kinzelbach 2001). After first coupling approaches between the FUB and GFZ numerical models, the geological and numerical models were completely revised and a newer version of ModFlow (ModFlow 2005) was used for the numerical model of the Cenozoic. After several convergence problems could be resolved, the different scenarios (chapter 4) were recalculated.

The coupling of the shallow hydrogeological model with the deep reservoir model was carried out using faults as potential migration pathways for formation fluids and by implementing mass flow rates, derived from the deep reservoir model, into the shallow hydrogeological model as so called Neumann flow boundary condition, considering the spatial distribution of saline water intrusion. Input data for the simulation of the pressure buildup within the shallow aquifers were gained from the calculated mass flow values by GFZ. The sum of the mass flow according to GFZ data, derived from a total of 15 fault elements of the deep structural model, was injected into layer 9 (aquifer 5) of the numerical model of the Cenozoic for the simulation of the pressure buildup within the upper layers.

In terms of modeling worst case scenarios, a gap within the Rupelian clay (layer 8) was implemented directly above the injection zone (Fig. 10).

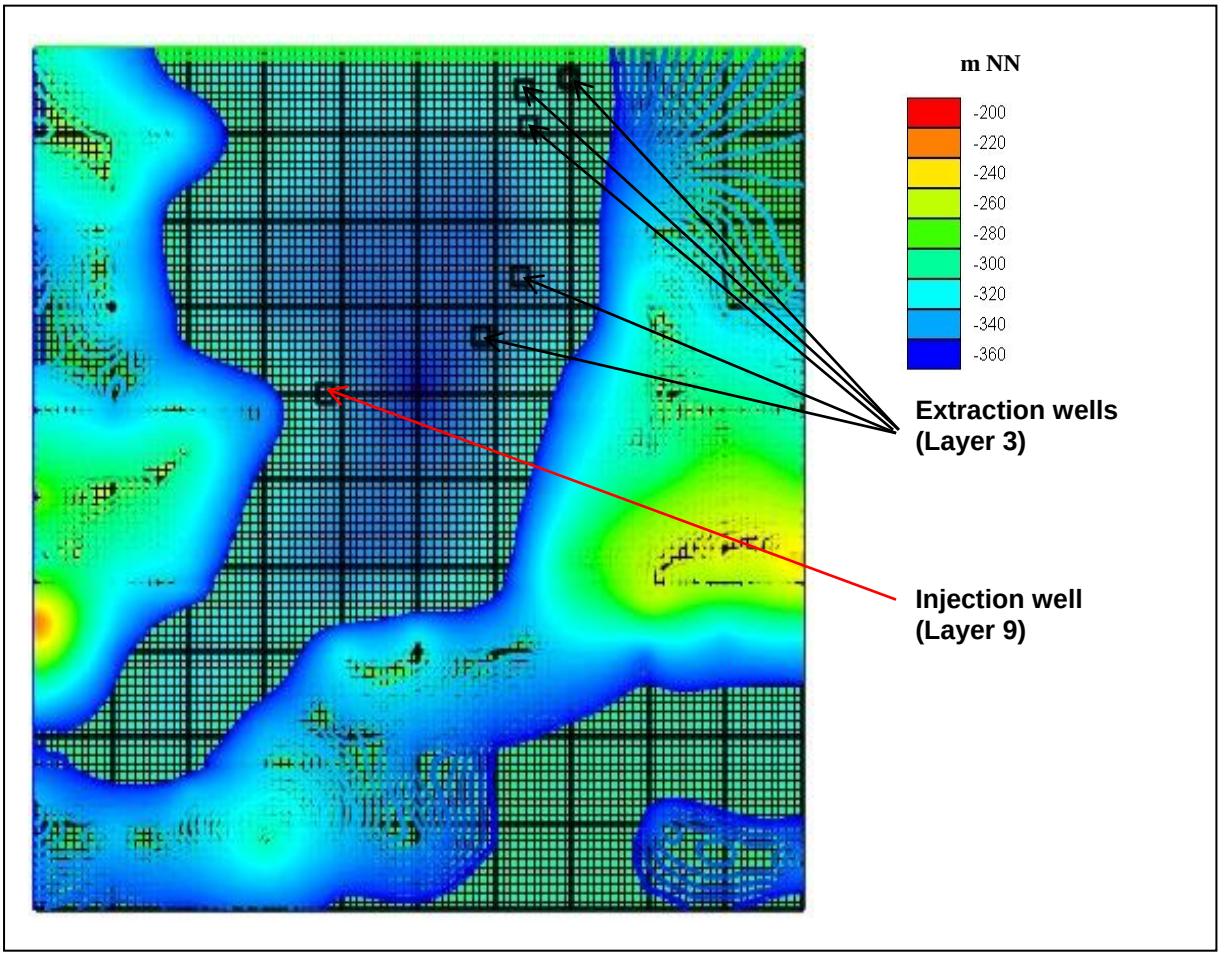

Fig. 10: Modflow implementation of the bottom of Rupelian clay with discontinuities (Layer 8 of the numerical model). Scale in m NN.

A total of 18 time steps or stress periods were simulated as follows (Tab. 4).

Tab. 4: Number of time steps (stress periods) and time since beginning of injection

Time step (stress period)	Time [days]	Time [years]
1	1	0.0027
2	5	0.0137
3	10	0.0274
4	25	0.0685
5	50	0.1370
6	100	0.2740
7	250	0.6849
8	500	1.3699
9	730	2
10	1825	5
11	2555	7
12	3650	10
13	5475	15
14	7300	20
15	7665	21
16	9344	25
17	21900	60
18	36500	100

For each time step, representing stress periods in the numerical model, the pressure buildup within every model-layer was calculated according to four different scenarios.

4 Scenario description and modelling results

Four different scenarios were calculated to determine the pressure buildup within the aquifers of the Cenozoic model. The data delivered from GFZ considered a laterally closed fault scenario as a worst case scenario and an laterally open fault scenario as an average case scenario (chapter 2.6). Both scenarios were calculated under the conditions of injection without water abstraction from the third layer and with a simulated water abstraction from layer 3 (aquifer 2) for drinking water supply.

Mass flow data of water and sodium chloride for the different scenarios, as delivered from simulations of the GFZ model, are shown in Fig. 11.

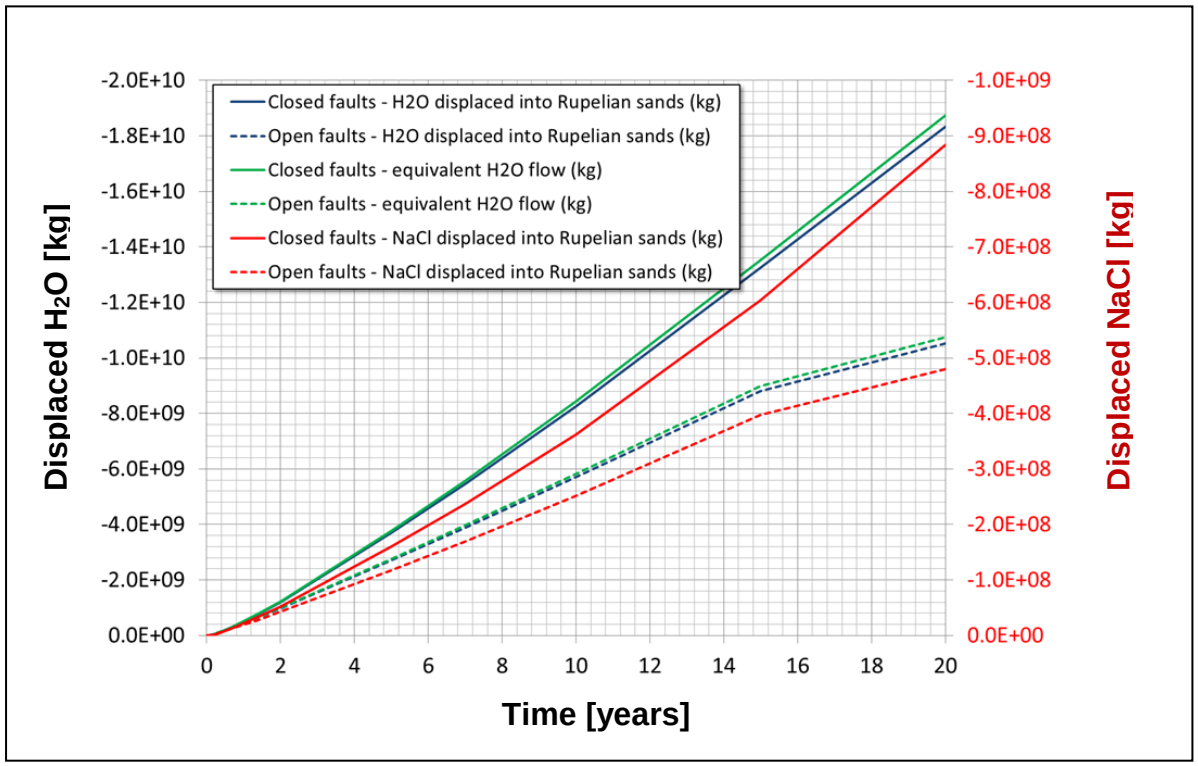

Fig. 11: Amount of displaced H_2O and NaCl as well as NaCl as equivalent H_2O-flow [kg] for the closed faults and open faults scenario according to GFZ data.

4.1 Laterally closed faults – without water abstraction ("worst case")

The mass flow of water for each time step regarding the **worst case scenario** with closed faults, implemented in the deep structural geological model, is shown in Fig. 12. The total amount of the injected fluid is about 18 Mio m^3.

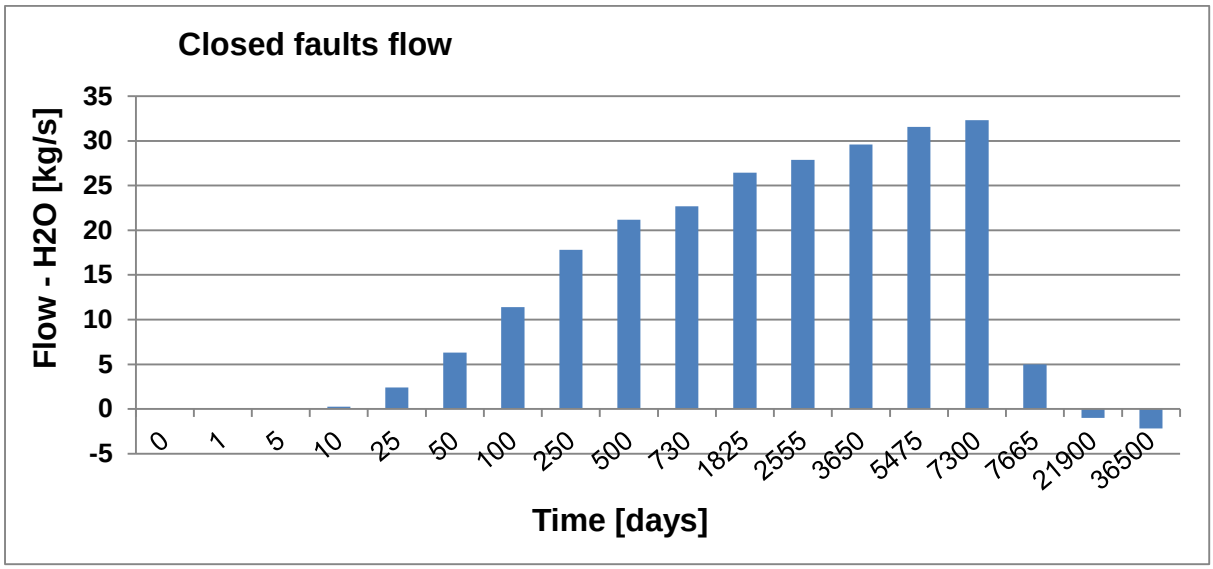

Fig. 12: Mass flow of H_2O into the layer beneath the Rupelian clay (layer 9) during a 20-year period of injection. Mass flow data derived from numerical simulation with laterally closed faults (worst case) using the deep structural geological model by GFZ.

The coupled flow of NaCl for the worst case scenario is shown in Fig. 13.

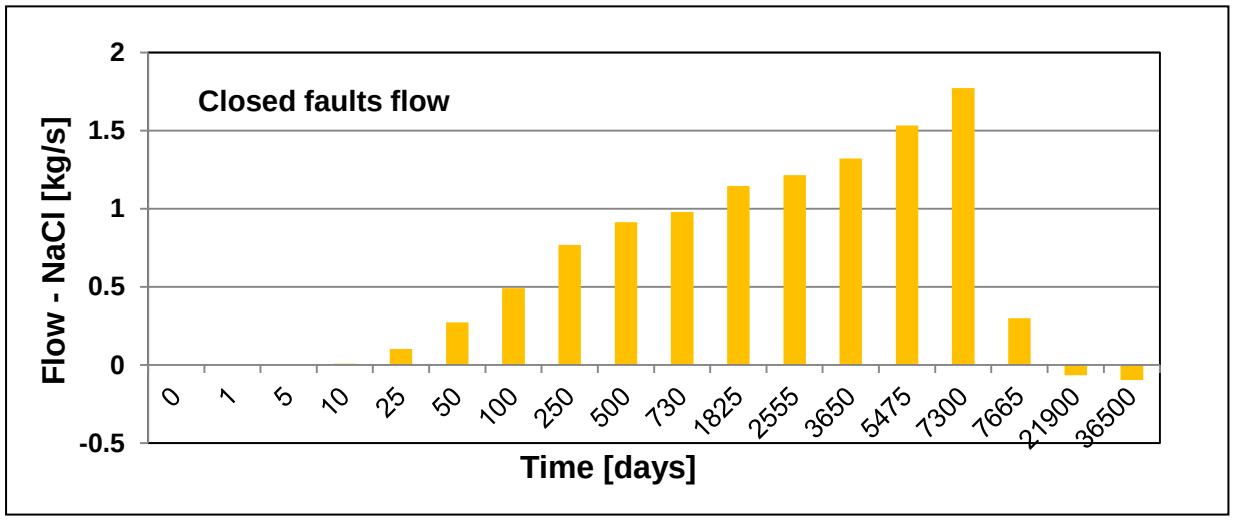

Fig. 13: Mass flow of NaCl into the layer beneath the Rupelian Clay (layer 9) during a 20-year period of injection. Mass flow data derived from numerical simulation with laterally closed faults (worst case) using the deep structural geological model by GFZ.

Fig. 14 shows the maximum pressure buildup within the aquifers over a time span of 20 years.

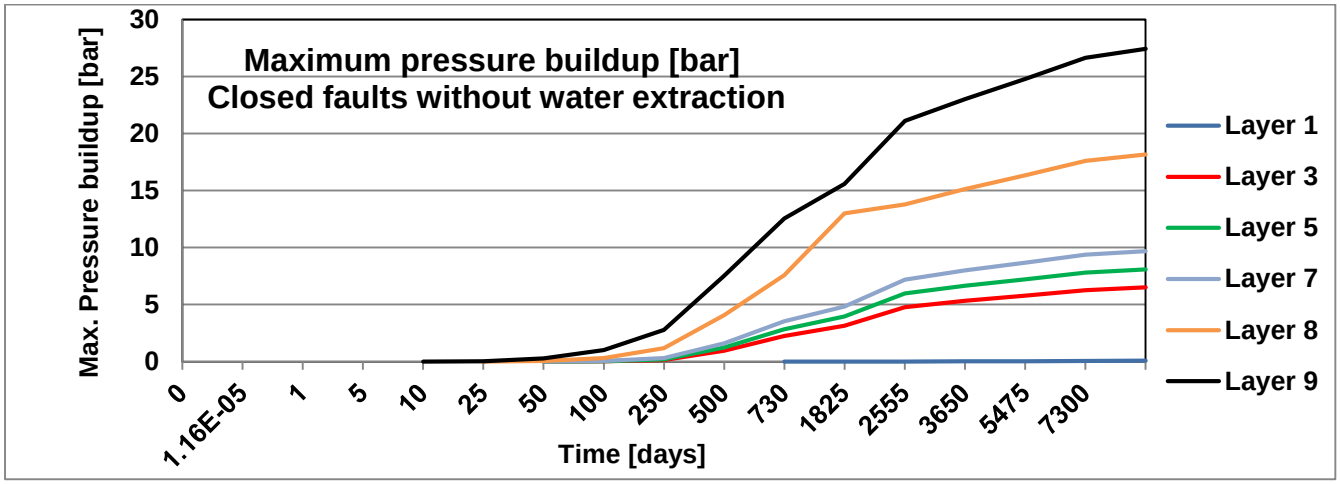

Fig. 14: Maximum pressure buildup [bar] within the relevant aquifers simulated for the worst case scenario with laterally closed faults, an injection period of 20 years and without water abstraction from layer 3.

4.2 Laterally closed faults – with water abstraction from Layer 3

The same scenario was simulated with an assumed water abstraction rate from layer 3 (aquifer 2) of 2.8 E-03 m^3/s (i.e. 10.08 m^3/h) per abstraction well (a typical pumping rate of an abstraction well in an urban area) over the total time span. The maximum pressure buildup for each aquifer is shown in Fig. 15.

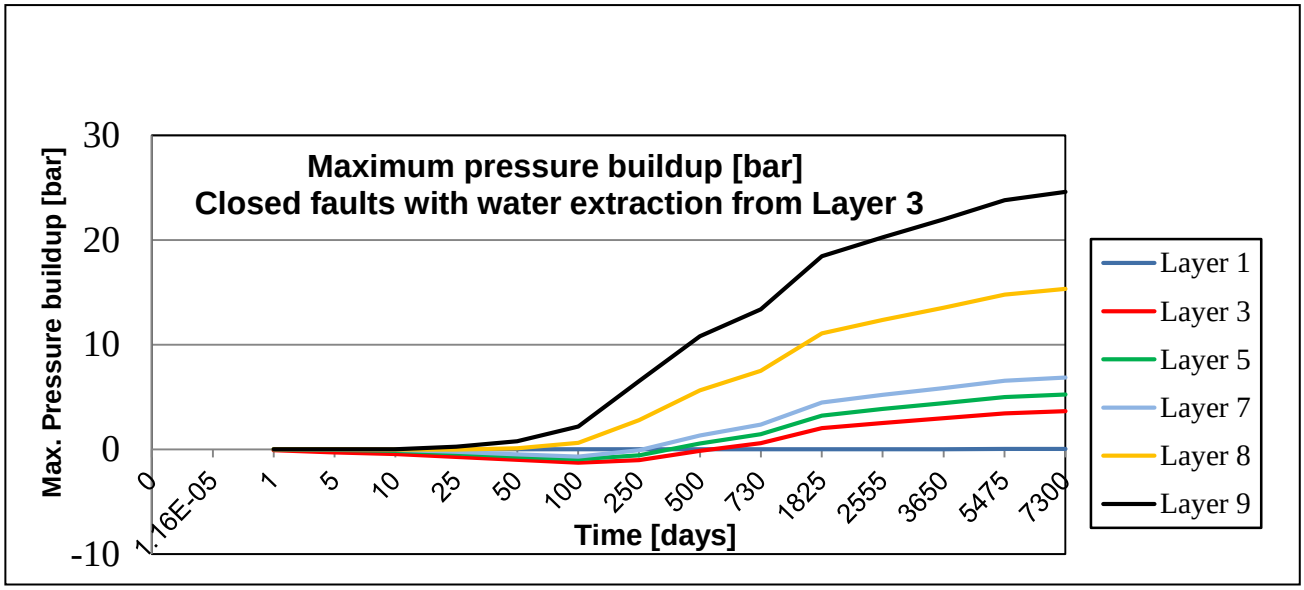

Fig. 15: Maximum pressure buildup [bar] within the relevant aquifers simulated for the worst case scenario with closed faults, an injection period of 20 years and water abstraction from layer 3 with an abstraction rate of 2.8 E-03 m^3/s (i.e. 10.08 m^3/h) per abstraction well.

4.3 Laterally open faults – without water abstraction ("average case")

The mass flow of water for each time step regarding the **average case scenario** with open faults, implemented in the deep structural geological model, is shown in Fig. 16. The total amount of the injected fluid is about 14 Mio m^3.

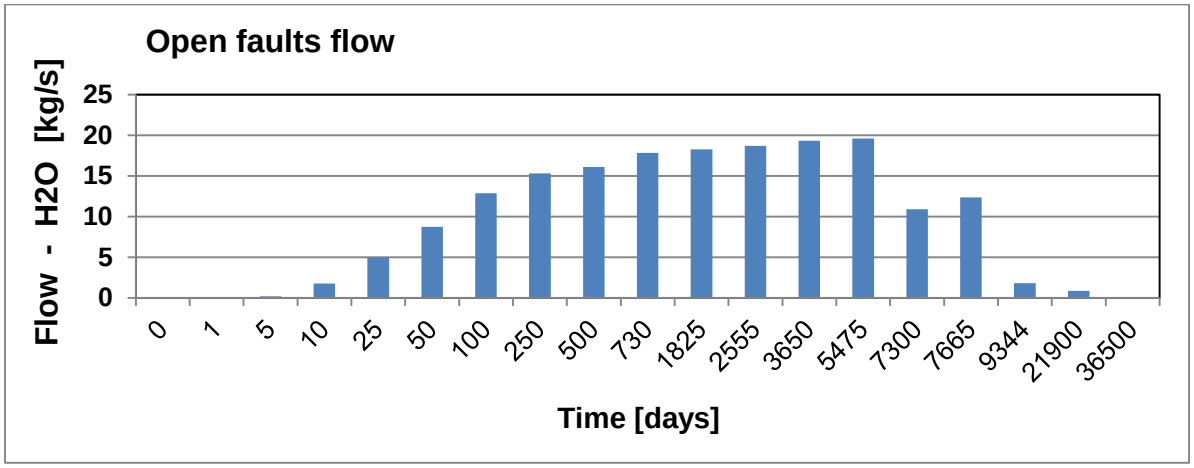

Fig. 16: Mass flow of H_2O into the layer beneath the Rupelian clay (layer 9) during a 20-year period of injection. Mass flow data derived from numerical simulation with laterally open faults (average case) using the deep structural geological model by GFZ.

The coupled flow of NaCl for the average scenario is shown in Fig. 17.

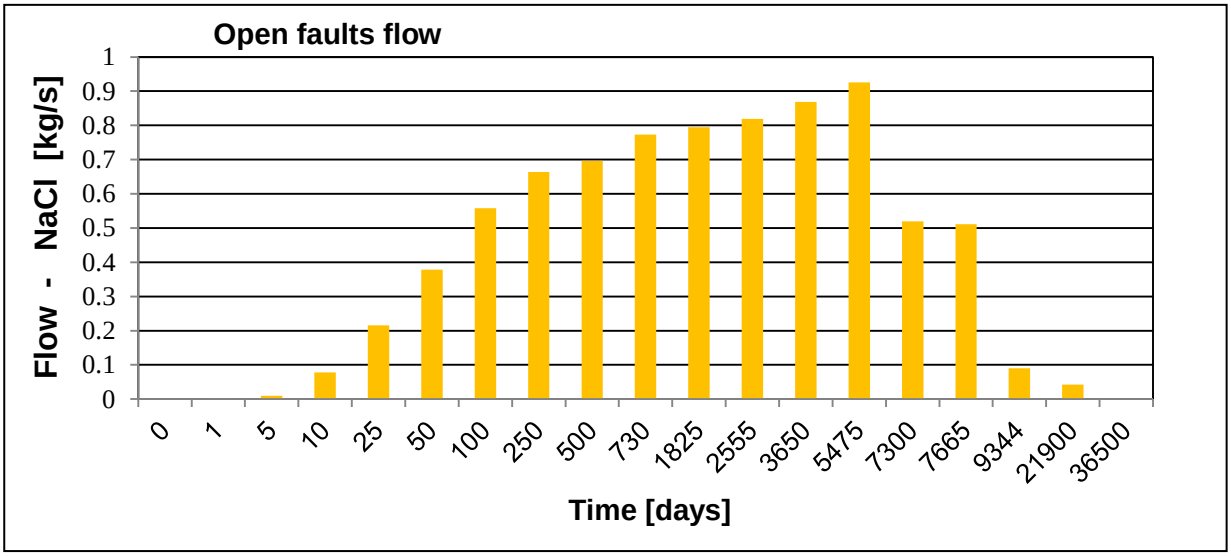

Fig. 17: Mass flow of NaCl into the layer beneath the Rupelian clay (layer 9) during a 20-year period of injection. Mass flow data derived from numerical simulation with laterally open faults (average case) using the deep structural geological model by GFZ.

Fig. 18 shows the maximum pressure buildup of the open faults scenario (average scenario) within the aquifers over a time span of 20 years without water abstraction from layer 3.

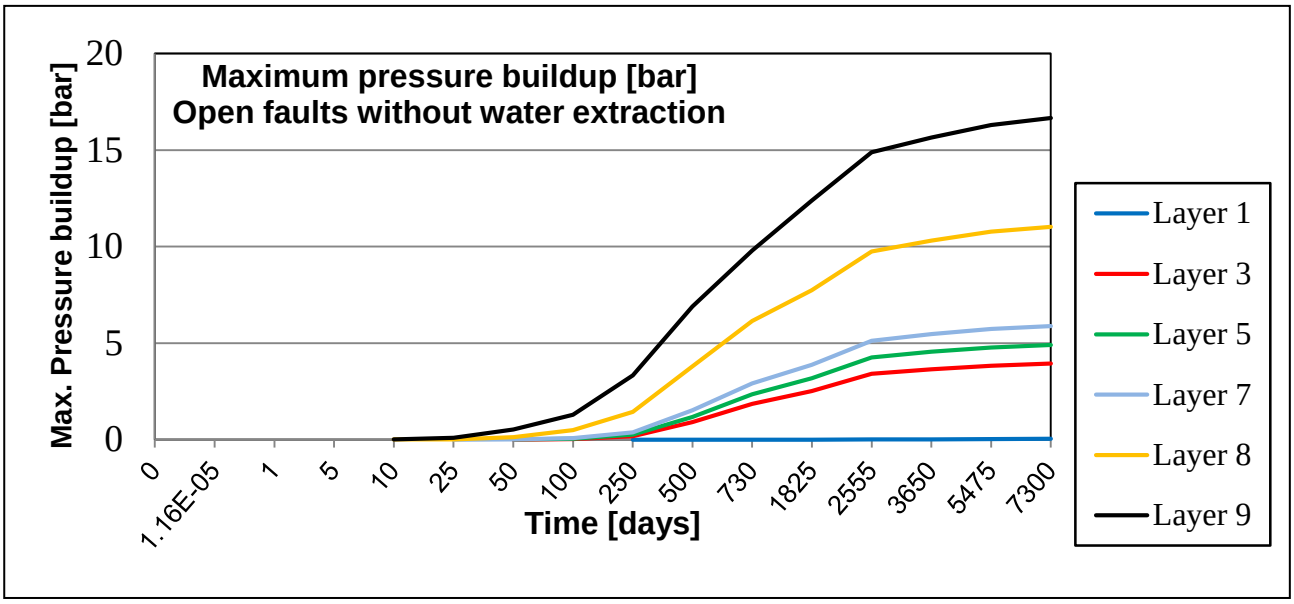

Fig. 18: Maximum pressure buildup [bar] within the relevant aquifers simulated for the average case scenario with laterally open faults, an injection period of 20 years and without water abstraction from layer 3.

4.4 Laterally open faults – with water abstraction from layer 3

The same scenario was simulated with an assumed water abstraction rate from layer 3 (aquifer 2) of 2.8 E-03 m^3/s (i.e. 10.08 m^3/h) per abstraction well (typical pumping rate of an abstraction well in an urban area) over the total time span. The maximum pressure build-up for each aquifer is shown in Fig. 19.

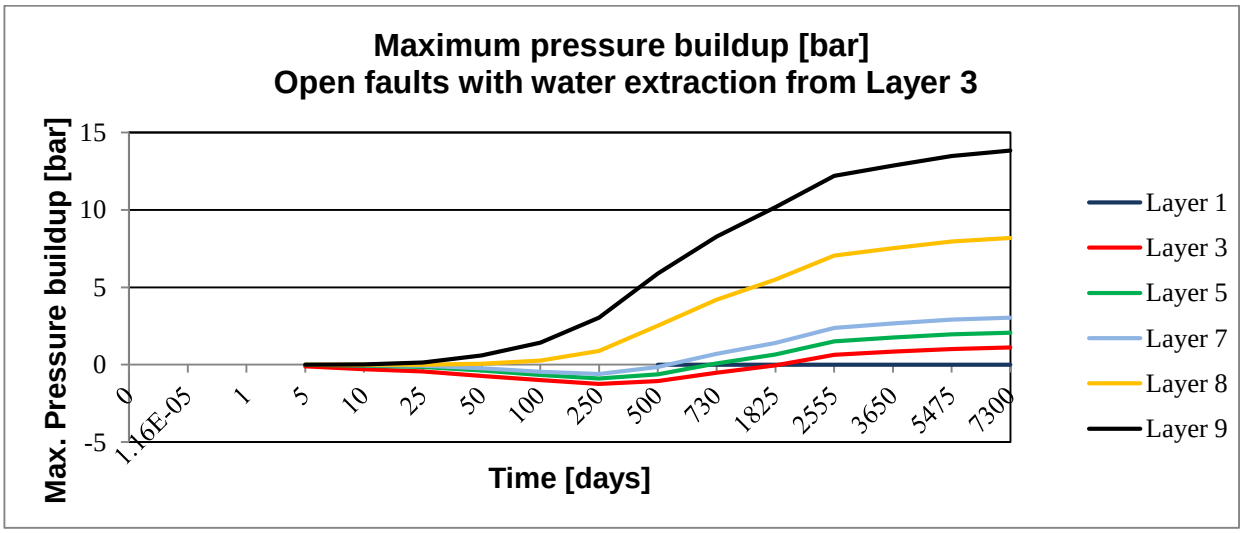

Fig. 19: Maximum pressure buildup [bar] within the relevant aquifers simulated for the average case scenario with laterally open faults, an injection period of 20 years and water abstraction from layer 3 with an abstraction rate of 2.8 E-03 m^3/s (i.e. 10.08 m^3/h) per abstraction well.

5 Interpretation of modelling results

Four different scenarios were modelled to estimate the pressure buildup within the aquifers of the Cenocoic model.

a) Laterally closed faults in the deep structural model ("worst case") without water abstraction from layer 3 (aquifer 2)
b) Laterally closed faults in the deep structural model ("worst case") with water abstraction from Layer 3 (aquifer 2)
c) Laterally open faults in the deep structural model ("average case") without water abstraction from layer 3 (aquifer 2)
d) Laterally open faults in the deep structural model ("average case") with water abstraction from layer 3 (aquifer 2)

In each scenario, the simulation results indicate a considerable and continuous pressure build-up within the injection horizon over the injection period of 20 years. The pressure build-up is slightly alleviated by a simultaneous water abstraction from layer 3 (aquifer 2) taking into account five abstraction wells with an abstraction rate of 2.8 E-03 m^3/s (i.e. 10.08 m^3/h) per well.

The **worst case scenario** without water abstraction shows a maximum pressure build-up up to 27 bar within the injection horizon (layer 9, i.e. aquifer 5) after 20 years of injection (Fig. 13).

The same scenario with water abstraction from layer 3 (aquifer 2) lowers the maximum pressure build-up in layer 9 to about 25 bar (Fig. 14).

After 20 years of injection, the maximum pressure build-up in layer 3, which is the main aquifer for drinking water production, is about 6.5 bar for the worst case scenario (Fig. 13) and about 3.7 bar in the case of water abstraction (Fig. 14).

The uppermost layer (aquifer 1) shows a pressure build-up of about 0.1 bar, which corresponds to a change of about 1 m in the groundwater surface. Water abstraction from layer 3 lowers this pressure build-up in layer 1 to about 0.04 bar or 0.4 m of rising groundwater.

In every scenario the pressure drops significantly after the end of injection and about 60-80 years later the system nearly reaches an equilibrium state with the natural pressure ratios prior to injection.

For the **average scenario** without water abstraction from layer 3, the maximum pressure build-up within the injection horizon (layer 9) is about 17 bar. In the case of continuous water abstraction of five abstraction wells with an abstraction rate of 2.8 E-03 m^3/s (i.e. 10.08 m^3/h) per well, the maximum pressure build-up is reduced to about 14 bar.

In both scenarios with continuous water abstraction from layer 3 (GWL 2), a dropdown of hydraulic heads is observed down to Layer 7 after 25 days of drinking water production. After 500 days in the worst case scenario and 1.5 – 5 years in the average case scenario, the influence of water production on hydraulic heads is counterbalanced by an increasing pressure build-up due to injection (Fig. 14 and 18). It is obvious that the different layers of the Cenozoic model react on positive and negative pressure pulses and that ascending saltwater can be expected both due to injection and abstraction from drinking water production wells.

Tab. 5 summarizes the simulation results of 20 years of injection. In both scenarios without water abstraction from layer 3, the maximum pressure build-up in layer 1 is reached with a time delay of 40-80 years after the end of injection. For every scenario, it is obvious, that the uppermost layer reacts with a remarkable delay in pressure build-up. Nevertheless the maximum change of hydraulic heads in layer 1 (GWL 1) is below 1 m (Tab. 5).

Tab. 5: Simulation results of 20 years of injection

Scenario	Boundary condition Cenocoic model	Boundary condition Deep structural model	Max. pressure buildup [bar]	Max. change of hydraulic heads [m]	(GWL / Layer)	Max. reached after ..... years
1	Closed (Neumann), without water abstraction from Layer 3	Laterally closed faults	0.09 6.5 8.1 9.7 18.2 27,4	0,9 65 81 97 182 274	(GWL 1 / Layer 1) (GWL 2 / Layer 3) (GWL 3 / Layer 5) (GWL 4 / Layer 7) (Rupelian/Layer 8) (GWL 5 / Layer 9 = injection horizon)	60 20 20 20 20 20
2	Closed (Neumann), with water abstraction from Layer 3	Laterally closed faults	0.04 3.7 5.2 6.9 15.3 24.6	0.4 36.6 52.5 68.5 153.3 246	(GWL 1 / Layer 1) (GWL 2 / Layer 3) (GWL 3 / Layer 5) (GWL 4 / Layer 7) (Rupelian/Layer 8) (GWL 5 / Layer 9 = injection horizon)	20 20 20 20 20 20
3	Closed (Neumann), without water abstraction from Layer 3	Laterally open faults	0.07 3.9 4.9 5.9 11.0 16.7	0.7 39.4 49 58.8 110 167	(GWL 1 / Layer 1) (GWL 2 / Layer 3) (GWL 3 / Layer 5) (GWL 4 / Layer 7) (Rupelian/Layer 8) (GWL 5 / Layer 9 = injection horizon)	100 20 20 20 20 20
4	Closed (Neumann), with water abstraction from Layer 3	Laterally open faults	0.009 1.1 2.1 3.0 8.2 13.8	0.09 11.1 20.7 30.5 82 138.3	(GWL 1 / Layer 1) (GWL 2 / Layer 3) (GWL 3 / Layer 5) (GWL 4 / Layer 7) (Rupelian/Layer 8) (GWL 5 / Layer 9 = injection horizon)	20 20 20 20 20 20

6 Discussion

This study describes the potential influence of CO_2 storage in deeper horizons on overlying geological structures, especially shallow aquifers, which are often used for drinking water production. Assuming that the injected CO_2 remains within the storage horizon, only pressure increase and distribution is relevant for adjacent geological structures. Similar concepts for modelling the pressure distribution in the course of CO_2 injection were developed by Birkholzer et al. (2009) and Schäfer et al. (2010).

Modelling showed that during the injection period the pressure increases rapidly within the storage horizon followed by a delayed pressure build-up in the overlying aquifers. At the end of the injection period of 20 years, the pressure drops significantly and nearly reaches the pressure ratios of those prior to injection after about 100 years, i. e. 80 years after injection has been stopped. Only layer 1 reacts with a time delay and reaches a maximum pressure build-up after 60-100 years but with changes in hydraulic heads below 1 m.

Because of the large time steps chosen and the limited lateral extent of the Cenozoic model, no spatial resolution of pressure heads within one layer could be depicted. Nevertheless, the simulation results have shown that the influence of CO_2 injection would reach far beyond the chosen extension of the Cenozoic model of 10 km x 10 km. Further simulation approaches should be realised with increased model dimensions and smaller time-steps.

The simulations, carried out as worst case scenarios, showed further, that due to a pressure build-up especially within the deeper aquifers, an upward migration of saltwater can be expected, influencing the quality of drinking water resources in layer 3 (GWL 2). To quantify the amount of saltwater introduced into shallow aquifers, further simulations regarding mass transport as well as density calculations and chemical reactions are required. For that purpose, calculation tools like MT3DMS or SEAWAT are recommended.

For a similar model, Schäfer et al. (2010) described substantial differences of pressure distribution between simulated open, semi-open and closed conditions. In their simulations, a pressure maximum is reached a few years after injection in all open or semi-open scenarios. On the other hand, all closed scenarios showed a pressure increase, even 30 years after the end of injection. In all simulations the injection was carried out with a single injection well into the storage horizon. Schäfer et al. (2010) pointed out, that in real injection operations a maximum of acceptable pressures should be determined and that the injection rate must be adapted to a maximum storage security.

Furthermore, the most important parameters for pressure distribution are the boundary conditions. The simulations have shown that open boundary conditions lead to a lower pressure build-up than closed boundary conditions.

Moreover, published data (Schäfer et al. 2010, Birkholzer et al. 2009, Kempka et al. 2013) show a significant influence of the compressibility and permeability of the different formations on pressure distribution.

Generally, elevated pressure in the storage formation may cause upward saltwater migration into shallow aquifers if vertical hydraulic conductivities are high enough and discontinuities in the Rupelian clay exist. Rising water tables can also lead to changes in discharge and recharge zones and can affect water quality in drinking water aquifers (Birkholzer et al. 2009).

Former studies with similar model setups but a wider lateral extent with a radius of 200 km around the injection zone, carried out by Birkholzer et al. (2009) showed that pressure buildup due to CO_2 injection can extend from the injection zone to a lateral radius of 100 km and through the entire vertical sequence up to the uppermost aquifer. They observed a pressure increase of 0.1 bar extending almost 85 km laterally within the storage formation and a pressure buildup of 2 bar, equal to a 20 m increase in piezometric head, at a radial extent of 45 km. In that case, the influence of pressure buildup covered an area of 22,000 km^2, compared to the CO_2 plume of only about 2 km radial extent. The pressure increase in the uppermost layer, simulated as a confined unit, was about 0.2 – 1.1 bar for the cases with the highest seal permeabilities of 10^{-17} and 10^{-16} m^2, corresponding to changes in hydraulic heads of 2 m and 11 m (Birkholzer et al. 2009).

Although the Cenozoic model of the COSMA project has a smaller lateral extent (10 km x 10 km), the range of pressure increase near the injection zone and within the storage horizon as well as the observed changes in hydraulic heads are in good accordance with the studies mentioned above. Taken into account a leakage of the Rupelian clay as sealing unit in that model, for the worst case scenario, vertical migration of saline water towards shallow aquifers is a reasonable concern.

Pore compressibility may decrease the theoretical increase in the hydraulic head resulting from a pressure increase in a deep saline aquifer. Moreover, initial salinity in the hydraulically conductive faults as well as in overlying saline aquifers is determining the degree of shallow groundwater salinization in addition to the effective fault porosity, since a volumetric assessment of saline water displacement has to be carried out when accounting for brine upward migration.

7 Summary

Based on literature research, hydrogeological profiles and borehole logs, a simplified hydrogeological model of the Cenozoic was created, representing the geological situation of the Northern German Sedimentary Basin, which was transferred to a numerical model using the finite difference computer code Modflow. The hydrogeological model should represent a "worst case" scenario, which includes windows within the Rupelian clay as well as deep glacial erosion channels which allow an ascent of salt water into the shallow freshwater aquifers. Therefore, the model does not represent the real situation within the deeper subsurface of a defined location, but possible geological conditions in the sense of worst-case scenarios.

Mass flow data, derived from the deep structural model of the GFZ, were used as input data for determining the injection rate into layer 9 of the Cenozoic model over an injection period of 20 years in order to simulate the pressure distribution in the different layers over various time steps.

Four scenarios were simulated to assess the pressure buildup within the aquifers due to CO_2 injection:

a) A worst-case scenario with laterally closed faults in the deep structural model without water abstraction from layer 3 (aquifer 2)
b) A worst-case scenario with laterally closed faults in the deep structural model with water abstraction from layer 3 (aquifer 2)
c) An average case scenario with laterally open faults in the deep structural model without water abstraction from layer 3 (aquifer 2)
d) An average case scenario with laterally open faults in the deep structural model with water abstraction from layer 3 (aquifer 2).

In each scenario, the simulation results indicate a considerable and continuous pressure build-up within the injection horizon over the injection period of 20 years, but the pressure drops significantly after the end of injection and about 60-80 years after injection the system nearly reaches an equilibrium state with the natural pressure ratios prior to injection. Only in layer 1, the maximum pressure build-up is reached after 60 years in the closed faults and 100 years in the open faults scenario, both calculated without water abstraction from layer 3. Nevertheless, the maximum change in hydraulic heads in layer 1 is always below 1 m.

For both scenarios, the worst-case and the average-case scenario, it is obvious, that simultaneous water abstraction can diminish the pressure increase in all model layers.

Therefore, a combined production of water, e.g. for use of geothermal energy, together with CO_2 injection activities could prevent undesirable effects of pressure increase.
Moreover, the modelling results suggest, that an upward migration of saltwater can be expected, due to a pressure build-up especially within the deeper aquifers, what possibly influences the quality of drinking water resources in layer 3 (GWL 2). To quantify the amount of saltwater introduced into shallow aquifers, further simulations regarding mass transport as well as density calculations and chemical reactions would be necessary. Therefore, other calculation tools like MT3DMS or SEAWAT could be used.

It has been shown, that modelling of the pressure distribution in different aquifers of the Cenozoic is possible using a coupling method considering the mass flow, derived from a separate underground utilization model, which has incorporated the main geological features present in the deeper underground, especially those of the CO_2 storage horizon.
Simulations of pressure distribution in different aquifers are a valuable tool for reservoir management, observation of pressure increase and planning of injection strategies. For real injection projects, site-specific modelling in due consideration of local hydrogeological conditions is required to carry out adequate risk assessments.
In accordance with other studies, it was found, that the main parameters for pressure simulations are model boundaries (open or closed), permeabilities and compressibility of the modelled layers, which has an influence on the storage capacity.

8 References

Birkholzer, J. T., Zhou, Q. & Tsang, C.-F. (2009): Large-scale impact of CO_2 storage in deep saline aquifers: A sensitivity study on pressure response in stratified systems.- Int. J. Greenhouse Gas Control, 3: 181-194.

Brink, H.-J. (2005): The evolution of the North German Basin and the metamorphism of the lower crust. *Int J Earth Sci (Geol Rundsch) 94*, S. 1103-1116.

Chiang, W.-H. & Kinzelbach, W. (2001): 3D-Groundwater Modeling with PMWIN – A Simulation System for Modeling Groundwater Flow and Pollution. Springer-Verlag Berlin, Heidelberg, New York, 346 S.

Franz, M. (2008): Litho- und Leitflächenstratigraphie, Chronostratigraphie, Zyklo- und Sequenzstratigraphie des Keupers im östlichen Zentraleuropäischen Becken (Deutschland, Polen) und Dänischen Becken (Dänemark, Schweden). *Dissertation, Martin-Luther-Universität Halle-Wittenberg*, 266. (in German)

Frey W. (1975): Zum Tertiär und Pleistozän des Berliner Raums.- Zeitschrift der deutschen geologischen Gesellschaft, (126), S. 281-292

Gocht W. (1964): Die Bedeutung des Septarientons für die Wasserversorgung Berlins.- Bohrtechnik und Brunnenbau, (15), S. 139-150, Berlin.

Harbaugh, A. W. (2005): MODFLOW-2005, The U.S. Geological Survey Modular Ground-Water Model - the Ground-Water Flow Process.- U.S. Geological Survey Techniques and Methods 6-A16, Reston, Virginia.

Kallenbach, H. (1980): Abriß der Geologie von Berlin.- In: Berlin. Klima, geologischer Untergrund und geowissenschaftliche Institute, Beilage zu den Tagungsunterlagen des Internationalen Alfred-Wegener-Symposiums und der Deutschen Meteorologen Tagung 1980, S. 15-21; Berlin.

Kallenbach, H. (1993): Zur Geologie von Berlin, Wirtschaftliche Nutzung und Ökologische Probleme.- Barbara Gespräche, Grenzen der Geotechnik , Payerbach 1993, S. 141-164, Wien.

Kempka, T., Herd, R., Huenges, E., Jahnke, C., Janetz, S., Jolie, E., Kühn, M., Magri, F., Möller, M., Munoz, G., Ritter, O., Schafrik, W., Schmidt-Hattenberger, C., Tillner, E., Voigt, H.-J. & Zimmermann, G. (2013): CO2-Speicherung in Ostbrandenburg: Implikationen für eine synergetische geothermische Energiegewinnung und Konzeptionierung eines Frühwarnsystems gegen Grundwasserversalzung - brine.- Endbericht Projekt brine, FKZ 03G0758A/B, Helmholtz-Zentrum Potsdam, Deutsches GeoForschungsZentrum (GFZ) Potsdam; Brandenburgische Technische Universität Cottbus; 125.

Kloos, R. (1986): Das Grundwasser in Berlin - Bedeutung, Probleme, Sanierungskonzeption.- Bes. Mitt. Gewässerkdl. Jh.- Ber. d. Landes Berlin, 165 S.; Berlin.

Kossow, D., Krawczyk, C., McCann, T., Strecker, M., & Negeendank, J. F. (2000): Style and evolution of salt pillows and related structures in the northern part of the Northeast German Basin. Int J Earth Sciences 89, S. 652-664.

Limberg, A. & Thierbach, J. (1997): Gliederung der Grundwasserleiter in Berlin. - Brandenburgische Geowiss. Beitr., 4, 2, S. 21 - 26, Kleinmachnow.

Limberg, A. & Thierbach, J. (2001): Hydrostratigrafie von Berlin - Korrelation mit dem Norddeutschen Gliederungsschema.- 7 S., Senatsverwaltung für Stadtentwicklung, Am Köllnischen Park 3, 10179 Berlin.

Limberg, A., Zech, A. & Stoltmann, N. (2009): Geologischer Atlas von Berlin.- SenGUV Berlin - Geologie und Grundwassermanagement.

Lippstreu, L. (1995): Brandenburg.- In: Benda, L. (Hrsg), Das Quartär Deutschlands, S. 116-147, Gebrüder Bornträger Verlag. Berlin.

Manhenke, V., Hannemann, M. & Rechlin, B. (1995): Gliederung und Bezeichnung der Grundwasserleiterkomplexe im Lockergestein des Landes Brandenburg. - Brandenburgische Geowiss. Beitr., Kurzmitteilung, 2, 1, S. 12, Kleinmachnow.

Manhenke, V., Reutter, E., Hübschmann, M., Limberg, A., Lückstedt, M., Nommensen, B., Peters, A., Schlimm, W., Taugs, R. & Voigt, H.-J. (2001): Hydrostratigrafische Gliederung des nord- und mitteldeutschen känozoischen Lockergesteinsgebietes. – Z. angew. Geol., 47, 3 u. 4, S. 146

McCann, T. (2008). The Geology of Central Europe: Precambrian and palaezoic. The Geo*logical Society of London*, 787.

Pekdeger, A, Sommer- von Jarmersted, C. & Kösters, E. (1998): Sicherung der Trinkwasser-versorgung Berlins - Hydrogeologische Voraussetzungen.- Abschlußbericht (unveröff.)

Pruess, K. (2005): ECO2N: A TOUGH2 Fluid Property Module for Mixtures of Water, NaCl, and CO2. Report LBNL-57952, Lawrence Berkeley National Laboratory, Berkeley, CA.

Röhmann, L., Tillner, E., Magri, F., Kühn, M. & Kempka, T. (2013). Fault reactivation and ground surface uplift assessment at a prospective German CO_2 storage site. *Energy Procedia EGU GA 2013 (* in press).

Schäfer, F., Walter, L., Class, H. & Müller, C. (2010): Regionale Druckentwicklung bei der Injektion von CO_2 in salinare Aquifere.- Projekt CO_2 - Drucksimulation, A-0602015.A, Abschlussbericht, Bundesanstalt für Geowissenschaften und Rohstoffe (BGR), Hannover, 58 S.

Scheck, M. & Bayer, U. (1999): Evolution of the Northeast German Basin - inferences from a 3D structural model and subsidence analysis. - Tectonophysics, 313, 1-2, 145-169.

Schlumberger (2011). Petrel Seismic-to-Evaluation Software, Version 2011.2.7.

Stackebrandt, W. (2009). Subglacial channels of Northern Germany - a brief review. *Z. dt. Ges. Geowiss. 160*, 203-210.

Stackebrandt, W., & Manhenke, V. (2004). Atlas zur Geologie von Brandenburg im Maßstab 1:1.000.000. *Landesamt für Geowissenschaften und Rohstoffe Brandenburg*, 143. (in German)

Szurlies, M. (2007): Latest Permian to Middle Triassic cyclo-magnetostratigraphy from the Central European Basin, Germany: Implications for the geomagnetic polarity timescale. *Earth and Planetary Science Letters 261*, S. 602-619.

Tesmer, M., Möller, P., Wieland, S., Jahnke, C., Voigt, H., & Pekdeger, A. (22. March 2007). Deep reaching fluid flow in the North East German Basin: origin and processes of groundwater salinisation. *Hydrogeology Journal 15*, S. 1291-1306.

Tillner, E., Kempka, T., Nakaten, B., & Kühn, M. (2013). Brine migration through fault zones: 3D numerical simulations for a prospective CO2 storage site in Northeast Germany. *Int. J. Greenhouse Gas Control* (in press) doi:10.1016/j.ijggc.2013.03.012.

Vattenfall (2009): Antrag auf Erteilung einer Erlaubnis zur Aufsuchung bergfreier Bodenschätze zu gewerblichen Zwecken. *http://www.lbgr.brandenburg.de/cms/detail.php/bb1.c.219232.de*, 12. (in German)

Vosteen, H.-D., Rath, V., Schmidt-Mumm, A., & Clauser, C. (2004, May 19). The thermal regime of the Northeastern-German Basin from 2-D inversion. *TECTONOPHYSICS-07179*, p. 15.

Williamson, M. M., & Hamilton, T. C. (1997). A Review of Zechstein Drilling Issues - Conference Paper. *Society of Petroleum Engineers*, 8.

Wurl, J. (1995): Die geologischen, hydraulischen und hydrochemischen Verhältnisse in den südwestlichen Stadtbezirken von Berlin.- Berliner Geowiss. Abh. (A), 172: 164S.; Berlin

Zhang, K., Wu, Y.-S. & Pruess, K. (2008). User's Guide for TOUGH2-MP – A Massively Parallel Version of the TOUGH2 Code. Report LBNL-315E, Earth Sciences Division, Lawrence Berkeley National Laboratory, Berkeley, CA.